Electronic Supplementary Material (ESI) for ChemComm.

Supplementary Information

A GLUTs/GSH cascade targeting-responsive bioprobe for the detection of circulating tumor cells

*Yi Wang, Jiahui Li, Zelong Chen, Liang Pu, Zhichao Pei and Yuxin Pei**

Shaanxi Key Laboratory of Natural Products and Chemical Biology, College of Chemistry & Pharmacy, Northwest A&F University

Yangling, Shaan Xi 712100, P. R. China

**Corresponding Author: Yuxin Pei*

E-mail address: peiyx@nwafu.edu.cn

Experimental section

Materials and instruments

Materials. All reagents were analytical grade unless otherwise noted and purchased from commercial suppliers and used without further purification. Water used in this work was ultrapure water. 2,3,4,6-tetra-O-acetyl-alpha-D-glucopyranosyl bromide, 4-(diethylamino)salicylaldehyde, diethyl malonate, sodium hydroxide, copper sulfate pentahydrate, copper(II) perchlorate hexahydrate and imidazole-2-carboxaldehyde were purchased from Adamas Chemical Reagent Co. Potassium carbonate, copper sulfate pentahydrate and acetic acid were purchased from Chron Chemical Reagent Co. Tosyl chloride, sodium methylate and sodium ascorbate were purchased from Aladdin Chemical Reagent Co. Sodium hydride and bis[2-(2-hydroxyethoxy)ethyl] ether were purchased from Xiya Chemical Reagent Co. Hydrazine monohydrate was purchased from J&K Chemical Reagent Co. 3-Bromopropyne was purchased from Jiuding Chemical Reagent Co. Red plasma membrane fluorescent probe (1,1'-dioctadecyl-3,3,3',3'-tetramethylindodicarbocyanine,4-chlorobenzenesulfonate salt, DiD) was purchased from Shanghai BioScience Co., Ltd.

Instruments. The synthetic compounds were characterized with SHIMADZU AXIMA Confidence matrix-assisted laser desorption/ionization time of flight mass spectrometry (MALDI-TOF-MS) and nuclear magnetic resonance (NMR) spectrometer (Bruker, German). The residual signals from DMSO-d_6 (^{1}H: δ 2.50 ppm; ^{13}C: δ 39.52 ppm) or $CDCl_3$ (^{1}H: δ 7.26 ppm; ^{13}C: δ 77.00 ppm) were used as internal standards. All fluorescence data measurements were obtained using a Shimadzu spectrometer (Japan) equipped with quartz cuvettes of 1 cm path length, and the UV-vis spectra were obtained on a Shimadzu 1750 UV-visible spectrophotometer (Japan). All pH buffer solutions were prepared on pB-10 digital pH meter (Sartorius, German). Cell fluorescent images were captured with a confocal laser scanning microscopy (Revolution WD, Andor). The detection of CTCs was conducted using a Flow cytometry (Beckman, USA).

Synthesis and characterization of GluCC

The detailed synthetic route and characterization about GluCC are described in Scheme S1 and Fig. S1-S16.

Compound **1** and **2** were synthesized *via* a published method [1].

Compound **1**: Diethyl malonate (1 mL, 6.5 mmol) and piperidine (0.4 mL) were added to 4-(diethyl amino) salicylic aldehyde (955 mg, 5.0 mmol) ethanol (3.3 mL) solution. The reaction mixture was stirred at room temperature for 2 hours. Then the mixture was diluted with water (50 mL) and extracted with ethyl acetate (50 mL × 3). The combined organic phase was dried over Na_2SO_4 and evaporated to dryness. Finally, **1** was purified by flash column chromatography on silica to give yellow solid, yield 93%. ^{1}H NMR (400 MHz, $CDCl_3$) δ 8.41 (s, 1H), 7.34 (d, J = 8.9 Hz, 1H), 6.59 (dd, J = 8.9, 2.5 Hz, 1H), 6.44 (d, J = 2.5 Hz, 1H), 4.36 (q, J = 7.1 Hz, 2H), 3.43 (q, J = 7.1 Hz, 4H), 1.38 (t, J = 7.1 Hz, 3H), 1.22 (t, J = 7.1 Hz, 6H) ppm.

Compound **2**: **1** (929 mg, 3.2mmol) was dissolved in anhydrous EtOH (9 mL). To this stirring solution, hydrazine monohydrate (0.622 mL, 12.8 mmol) was added. The reaction mixture was stirred at room temperature until no further precipitate was observed, at which point it was cooled to 0 ºC and stirred for another 15 min. The precipitate was collected via vacuum filtration and purified by flash column chromatography on silica to give yellow solid, yield 81%. ^{1}H NMR (500 MHz, $CDCl_3$) δ 9.70 (s, 1H), 8.67 (s, 1H), 7.42 (d, J = 8.9 Hz, 1H), 6.68 – 6.61 (m, 1H), 6.49 (s, 1H), 4.13 (s, 2H), 3.45 (q, J = 7.1 Hz, 4H), 1.23 (t, J = 7.1 Hz, 7H) ppm.

Compound **3** and **4** were synthesized according to the published procedure [2].

Compound **3**: 2,3,4,6-tetra-O-acetyl-alpha-D-glucopyranosyl bromide (2.042g, 5.0 mmol) and sodium azide (468 mg, 7.2 mmol) were added into dimethyl sulfoxide (10 mL). The reaction mixture was stirred for 10 minutes at room temperature. Then the mixture was diluted with water (30 mL) and extracted with dichloromethane. The combined organic phase was washed with brine twice, dried over anhydrous Na_2SO_4 and evaporated to dryness to give colorless oil, yield %. ^{1}H NMR (400 MHz, $CDCl_3$)

δ 5.22 (t, J = 9.5 Hz, 1H), 5.11 (t, J = 9.7 Hz, 1H), 4.96 (t, J = 9.2 Hz, 1H), 4.65 (d, J = 8.9 Hz, 1H), 4.28 (dd, J = 12.5, 4.7 Hz, 1H), 4.17 (dd, J = 12.5, 2.3 Hz, 1H), 3.80 (ddd, J = 10.0, 4.8, 2.3 Hz, 1H), 2.06 (dd, J = 28.1, 9.4 Hz, 12H) ppm.

Compound **4**: CH_3ONa (80 mg, 1.5 mmol) was added into the solution of **3** (403 mg, 1.0 mmol) in methanol (10 mL). The reaction mixture was stirred at room temperature for 2 hours and then neutralized by addition of ion-exchange resin (Amberlite IR 120 H^+) until pH = 7. The mixture was filtered and the solvent was evaporated to dryness to give colorless solid, yield 86%. ^{1}H NMR (400 MHz, DMSO-d_6) δ 5.53 (d, J = 94.7 Hz, 2H), 4.76 (s, 1H), 4.44 (d, J = 8.6 Hz, 1H), 3.66 (dd, J = 12.0, 2.0 Hz, 1H), 3.48 – 3.42 (m, 1H), 3.24 – 3.12 (m, 3H), 3.06 (t, J = 9.2 Hz, 1H), 2.97 (t, J = 8.8 Hz, 1H) ppm.

Compound **5** and **6** were synthesized according to the published procedure [3].

Compound **5**: Tetra (ethylene glycol) (19.56 g, 100.8 mmol) was dissolved in THF (40 mL) followed by adding NaH (2.41 g, 50.4 mmol) at 0 ℃. Then 3-bromopropyne (1.77 g, 14.85 mmol) was dissolved in THF (7.5 mL) and added dropwise into the mixture at 0 ℃. The reaction mixture was stirred at room temperature for 2 hours, then diluted with water (50 mL). The THF was evaporated in vacuum. The aqueous solution was extracted with dichloromethane (100 mL × 3). The combined organic phase was dried over Na_2SO_4 and evaporated to dryness to give pale yellow oil, yield 87%. ^{1}H NMR (400 MHz, $CDCl_3$) δ 4.20 (d, J = 2.4 Hz, 2H), 3.74 – 3.64 (m, 14H), 3.63 – 3.58 (m, 2H), 2.43 (t, J = 2.4 Hz, 1H), 2.04 (s, 1H) ppm.

Compound **6**: NaOH (1.5 g, 37.5 mmol) in water (15 mL) was added into the solution of **5** (2.993 g, 12.9 mmol) and Tosyl chloride (4.15 g, 21.8 mmol) in THF (35 mL) under 0 ℃. The reaction mixture was stirred at room temperature for 2 hours and then evaporated in vacuum. The crude product was purified by flash column chromatography on silica to give colorless oil, yield 92%. ^{1}H NMR (400 MHz, $CDCl_3$) δ 7.79 (d, J = 8.4 Hz, 2H), 7.36 – 7.31 (m, 2H), 4.19 (d, J = 2.4 Hz, 2H), 4.18 – 4.12 (m, 2H), 3.71 – 3.55 (m, 14H), 2.44 (s, 3H), 2.42 (t, J = 2.4 Hz, 1H) ppm.

Compound **7**: **6** (1.55 g, 4.0 mmol), imidazole-2-carboxaldehyde (423 mg, 4.4 mmol), and K_2CO_3 (829 mg, 6.0 mmol) were added into dry DMF (20 mL). The reaction mixture was refluxed for 18 hours under 110 ℃ and then diluted with water (20 mL). The mixture was extracted with ethyl acetate and the combined organic phase was evaporated in vacuum. The crude product was purified by flash column chromatography on silica to give colorless oil, yield 58%. ^{1}H NMR (400 MHz, $CDCl_3$) δ 9.80 (s, 1H), 7.36 (s, 1H), 7.27 (s, 1H), 4.61 (t, J = 5.0 Hz, 2H), 4.20 (d, J = 2.5 Hz, 2H), 3.78 (t, J = 5.0 Hz, 2H), 3.69 (d, J = 3.6 Hz, 4H), 3.63 (d, J = 3.7 Hz, 4H), 3.58 (s, 4H), 2.45 (s, 1H) ppm. ^{13}C NMR (101 MHz, $CDCl_3$) δ 182.17, 142.96, 131.40, 127.94, 79.60, 74.61, 70.59, 70.54, 70.51, 70.44, 70.39, 70.05, 69.08, 58.38, 47.47 ppm. MS (ESI) $C_{15}H_{22}N_2O_5$ calc. for $[M+H]^+$, 311.1602, found 311.1591; for $[M+H+CH_3OH]^+$, 343.1864, found 343.1855.

Compound **8**: The solution of $CuSO_4 \cdot 5H_2O$ (52 mg, 0.2 mmol) and sodium ascorbate (208 mg, 0.7 mmol) in water (4 mL) was added into the solution of **4** (239 mg，1.2 mmol) and **7** (593 mg, 1.9 mmol) in water (13 mL) and THF (11 mL). The reaction mixture was stirred at room temperature for 24 hours and then evaporated in vacuum. The crude product was purified by flash column chromatography on silica to give colorless oil, yield 46%. ^{1}H NMR (400 MHz, DMSO-d_6) δ 9.69 (s, 1H), 8.29 (s, 1H), 7.67 (s, 1H), 7.31 (s, 1H), 5.52 (d, J = 9.2 Hz, 1H), 5.42 (d, J = 5.8 Hz, 1H), 5.33 (d, J = 4.7 Hz, 1H), 5.20 (d, J = 5.3 Hz, 1H), 4.67 (t, J = 5.5 Hz, 1H), 4.52 (s, 4H), 3.82 – 3.63 (m, 4H), 3.60 – 3.51 (m, 4H), 3.45 (q, J = 9.0, 7.4 Hz, 11H), 3.23 (dt, J = 13.8, 6.9 Hz, 1H) ppm. ^{13}C NMR (101 MHz, DMSO-d_6) δ 182.38, 144.30, 131.45, 129.04, 123.64, 87.92, 80.39, 77.39, 72.52, 70.23, 70.15, 70.09, 70.05, 69.99, 69.70, 69.55, 63.87, 61.19, 55.40, 49.07, 47.05 ppm. MS (ESI) $C_{21}H_{33}N_5O_{10}$ calc. for $[M+H]^+$, 516.2300, found 516.2291; for $[M+Na]^+$, 538.2119, found 538.2098; for $[M+H+CH_3OH]^+$, 548.2562, found 548.2539.

GluC: **8** (243 mg, 0.5 mmol) and **2** (136 mg, 0.5 mmol) were dissolved in methanol (8 mL) followed by adding a drop of acetic acid. The reaction mixture was stirred at room temperature for 5 hours and then evaporated in vacuum. The crude product was

purified by flash column chromatography on silica to give yellow solid, yield 90%. ^{1}H NMR (400 MHz, $CDCl_3$) δ 14.90 (s, 1H), 8.72 (s, 1H), 8.07 (s, 1H), 7.67 (s, 1H), 7.42 (s, 1H), 7.29 (s, 1H), 7.09 (s, 1H), 6.58 (d, J = 9.2 Hz, 1H), 6.39 (s, 1H), 5.70 (s, 1H), 4.52 (s, 2H), 4.25 (s, 2H), 4.08 (s, 2H), 3.95 – 3.26 (m, 26H), 1.19 (t, J = 7.0 Hz, 6H). ^{13}C NMR (101 MHz, DMSO-d_6) δ 161.22, 159.39, 157.47, 152.85, 148.55, 143.86, 140.02, 131.88, 129.21, 128.58, 123.23, 122.73, 110.40, 108.50, 107.86, 96.00, 87.50, 79.98, 76.98, 72.11, 69.82, 69.75, 69.71, 69.67, 69.56, 69.50, 69.11, 63.44, 60.76, 46.58, 44.49, 44.44, 12.38 ppm. MS (ESI) $C_{35}H_{48}N_8O_{12}$ calc. for $[M+H]^+$, 773.3470, found 773.3452; for $[M+Na]^+$, 795.3284, found 795.3274.

GluCC: $Cu(ClO_4)_2 \cdot 6H_2O$ (37 mg，0.1 mmol) and GluC (77 mg，0.1 mmol) were dissolved in methanol (15 mL). The reaction mixture was refluxed for 2 hours under 80 ℃ and then evaporated in vacuum to give crimson solid, stoichiometrically. MS (ESI) $C_{35}H_{47}N_8O_{12}Cu^{2+}$ calc. for [M], 834.2604, found 834.2608.

General spectrum measurements

Stock solutions of bioprobe GluCC and relevant detection substrates were prepared in ultrapure water. The UV–vis and fluorescence emission spectra of GluCC were measured in 10.0 mm path length quartz cuvettes. Excitation was provided at 450 nm with excitation and emission slit widths of 5 nm.

Calculation of the dissociation constant

The dissociation constant (K_d) of GluCC was calculated from the fluorescence titration data by using the equation for 1:1 complex[4]:

$$F - F_{initial} = \frac{[Cu^{2+}](F_{final} - F_{initial})}{K_d + [Cu^{2+}]}$$

where F is the observed fluorescence intensity, F_{final} is the fluorescence intensity for the GluCC, and $F_{initial}$ is the fluorescence for the GluC. The K_d value was calculated to be 2.033 μM (R^2 = 0.9901).

Calculation of fluorescence quantum yields

Rhodamine 6G (QY = 95% in water) for the emission range of 480 - 560 nm was selected as the reference. The quantum yields of GluCC before and after the rection with GSH was then calculated according to the following equation:

$$\emptyset = \emptyset' \times \frac{A'}{I'} \times \frac{I}{A} \times \frac{n^2}{n'^2}$$

Where $\emptyset$ is the quantum yield of the testing sample, I is the testing sample's integrated emission intensity, n is the refractive index (1.33 for water), and A is the optical density. The superscript "′" refers to the referenced fluorescence dyes of known quantum yield.[5] Finally, the fluorescence quantum yields of GluCC and after the reaction with GSH (GluC) were calculated to be 0.018 and 0.036, respectively.

General cell culture

Human liver hepatocellular carcinoma HepG2, human cervical carcinoma HeLa, human colon cancer KM-12, human ovarian cancer SKOV-3, human chronic myelocytic leukemia K562, T-cell acute lymphoblastic leukemia Jurkat, human liver HL7702, human monocyte THP-1, and mouse breast cancer 4T1 cell lines were obtained from KeyGEN BioTECH Co. (Nanjing, China). HepG2, K562, Jurkat, 4T1, HL7702, and THP-1 cell lines were cultured in 1% (v/v) antibiotics and 10% (v/v) FBS supplemented Roswell Park Memorial Institute medium (RPMI 1640, Gibco) under 5% CO_2 at 37 °C. HeLa, KM-12, and SKOV-3 cells were cultured under the same conditions except Dulbecco's Modified Eagle Medium (DMEM, Gibco) was used.

Cytotoxicity assays

HepG2 cells were seeded into 96-well plates at the density of 5×10^3 cells/well containing 100 μL complete 1640 medium and cultured for 24 h. Subsequently, the medium in the well was removed. GluCC at the doses of 0.05, 0.1, 0.5, 1, 5, and 10 μM in medium were added and cultured for 24 h and 48 h, respectively. The cell viability was evaluated using MTT assay.

Optimizing of GluCC working concentration

HepG2 cells were seeded into 35 mm plastic bottomed μ-dishes at the density of 10^5 cells/dish containing 1.5 mL complete 1640 medium and cultured for 24 h. Subsequently, the medium in the well was removed. GluCC at the doses of 10^0, 10^1, 10^2, 10^3, and 10^4 nM in medium were added and cultured for 30 min. The fluorescent images were obtained using CLSM with excitation at 445 nm and emission at 488 nm.

Photostability of GluCC in cancer cells

HepG2 cells were seeded into 35 mm plastic bottomed μ-dishes at the density of 10^5 cells/dish containing 1.5 mL complete 1640 medium and cultured for 24 h. Subsequently, the medium in the well was removed. GluCC at the doses of 10 μM in medium were added and observed under CLSM for 60 min with excitation at 445 nm and emission at 488 nm. Photos were captured every 4 min.

Intracellular localization of GluCC

HepG2 cells were seeded into 35 mm plastic bottomed μ-dishes at the density of 10^5 cells/dish containing 1.5 mL complete 1640 medium and cultured for 24 h. Subsequently, the medium in the well was removed. Cells cultured with 10 μM GluCC for 30 min and then cytomembrane was stained with DiD before observation under CLSM. For GluCC, λ_{ex} = 445 nm; for DiD, λ_{ex} = 644 nm.

Targeting ability and GSH responsiveness of GluCC towards cancer cells

HepG2 and HL7702 cells were seeded into 35 mm plastic bottomed μ-dishes at the density of 10^5 cells/dish containing 1.5 mL complete 1640 medium and cultured for 24 h. Subsequently, the medium in the well was removed. The cells were incubated with 10 μM GluCC in the culture media for 30 min and observed under CLSM with excitation at 445 nm and emission at 488 nm. For verification of GluCC targeting ability, HepG2 cells were pre-incubated with 0.2 mM phloretin for 1 h and then 10 μM GluCC for 30 min before observation. For verification of GluCC GSH responsiveness, HepG2 cells were pre-incubated for 30 min with 1 mM N-

ethylmaleimide (NEM, scavenger of GSH), and cleared with PBS 3 times, followed by adding 2 mM GSH and 10 μM GluCC for 30 min before observation.

The internalization pathway of GluCC

HepG2 cells were seeded into 6-well plates at the density of 2 × 10^5 cells/well containing 2 mL complete 1640 medium and cultured for 24 h. Subsequently, the medium in the well was removed. Cells were pre-incubated with sodium azide (10 mM), genistein (200 μg/ml), chlorpromazine (50 μg/mL) and phloretin (0.2 mM) at 37 °C for 1 h[6] and then cultured with GluCC at 37 °C for 30 min. The cells were then washed with PBS three times and digested to analyze the mean fluorescence intensity by flow cytometry.

Selective cancer cells imaging

HepG2, Hela, KM-12, SKOV-3, Jurkat, K562, HL7702, and THP-1 cells were seeded into 35 mm plastic bottomed μ-dishes at the density of 10^5 cells/dish containing 1.5 mL culture medium and cultured for 24 h. Subsequently, the medium in the well was removed. The cells were incubated with 10 μM GluCC in the culture media for 30 min and observed under CLSM with excitation at 445 nm and emission at 488 nm.

CLSM imaging of cancer cell spiked human peripheral blood samples

Different amount of Jurkat or K562 cells (with or without DiD marking) were spiked into 50 μL human peripheral blood without red blood cells (RBCs) (treated with ACK lysis buffer). Cells were incubated with 10 μM GluCC in the culture media for 30 min in 35 mm plastic bottomed μ-dishes and then imaged by CLSM. For GluCC, λ_{ex} = 445 nm; for DiD, λ_{ex} = 644 nm.

Flow cytometry for the detection of cancer cells spiked in human peripheral blood samples

Different amount of Jurkat or K562 cells (around 0.1% or 0.5%) were spiked into human peripheral blood without RBCs (treated with ACK lysis buffer). Cells were incubated with 10 μM GluCC in the culture media for 30 min in 12-well plates.

Fluorescence intensities from the gates of peripheral blood cells, Jurkat cells, K562 cells, Jurkat cells spiked peripheral blood cells and K562 cells spiked peripheral blood cells were recorded (with excitation at 405 nm). Data were analyzed with CytExpert software (Beckman, USA).

Detection of circulating tumor cells in peripheral blood of lung metastatic mouse model

Lung metastatic mouse models were built according to the references with some modification.[7] Owing to good biocompatibility and long retention time in cells (at least 30 days), DiD has been successfully applied in the *in vivo* tracing of many kinds of cells.[8] 4T1 cells were first cultured with 10 μM DiD in PBS for 40 min at 37 °C, 5% CO_2. Then 1×10^6 DiD labelled 4T1 cells in PBS were injected into the 4- to 6-week-old female Balb/c mice (purchased from Xi'an yifengda Biotechnology Co., Ltd) via the tail vein to generate a lung metastatic mouse model. The mice were sacrificed on day 18, 19, and 20, respectively. Lungs were immobilized with Bouin's solution overnight and stored in 70% ethanol and peripheral blood was collected using heparin sodium vacuum tube from mouse orbit. The blood cells were collected by centrifuge (400-500 g) for 5 min and then lysed red blood cells using ACK lysis buffer followed by PBS washing for 3 times. Then the collected cells were cultured with 10 μM GluCC in complete 1640 medium at 37 °C, 5% CO_2 for 30 min. After this, cells were washed with PBS for 3 times and then observed under CLSM. For GluCC, λ_{ex} = 445 nm; for DiD, λ_{ex} = 644 nm.

Animal care and handing procedures were approved by the Animal Care and Use Committee of Northwest A&F University (Shaanxi, China). Research programs involving animals are conducted in accordance with the approved guidelines. All animal procedures complied with all relevant ethical regulations and were approved by the Northwest A&F University Animal Care Committee (NWAFU-314020038).

Supplementary Figures

Synthesis of bioprobe GluCC

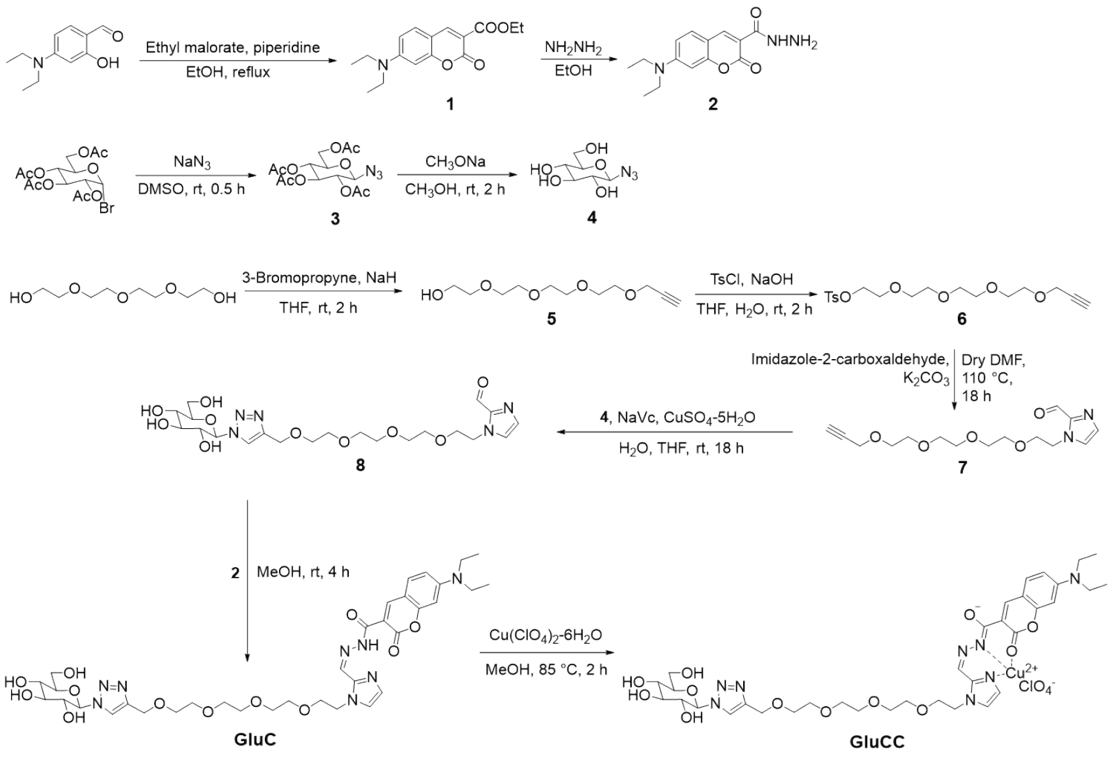

Scheme S1. Synthesis of bioprobe GluCC.

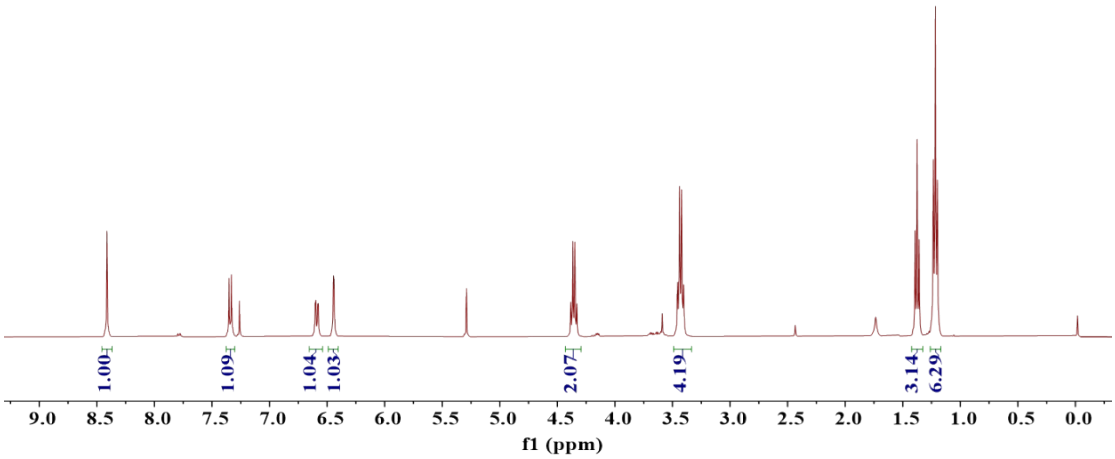

Fig. S1. ^{1}H NMR spectrum of **1** in $CDCl_3$.

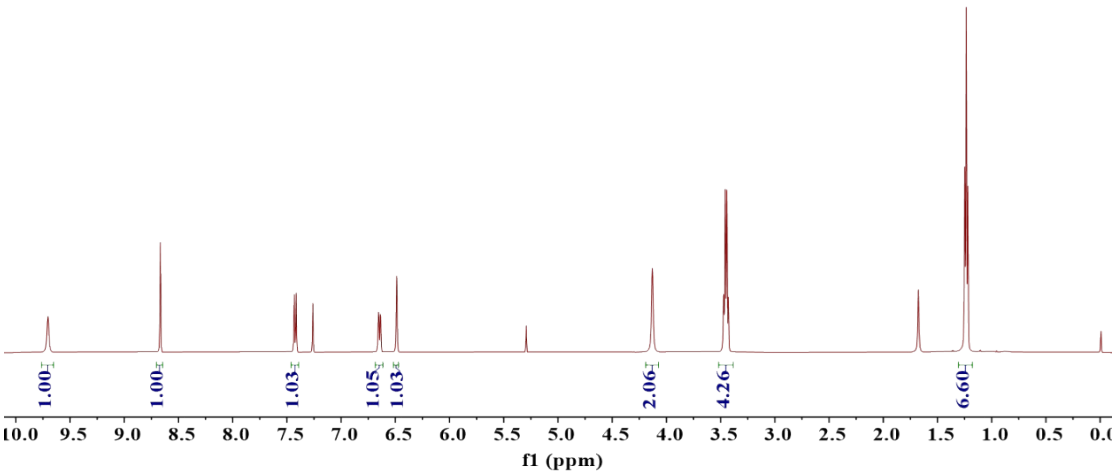

Fig. S2. ^{1}H NMR spectrum of **2** in $CDCl_3$.

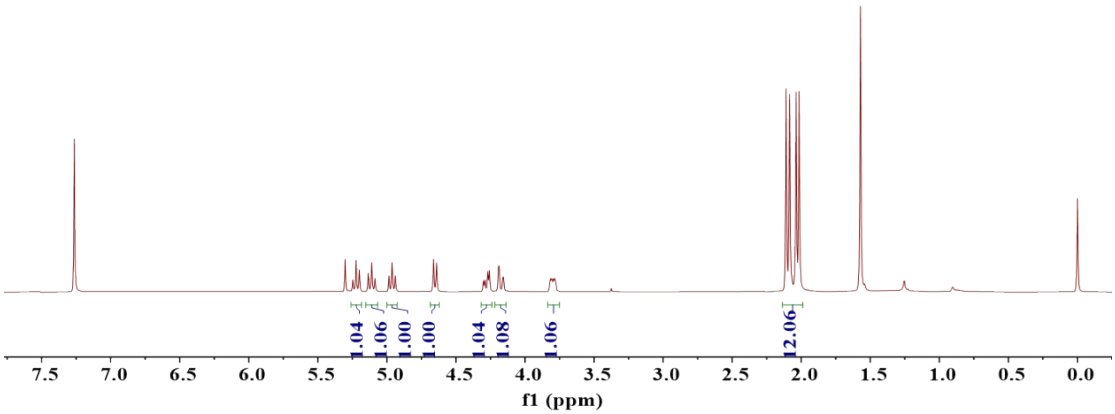

Fig. S3. ^{1}H NMR spectrum of **3** in $CDCl_3$.

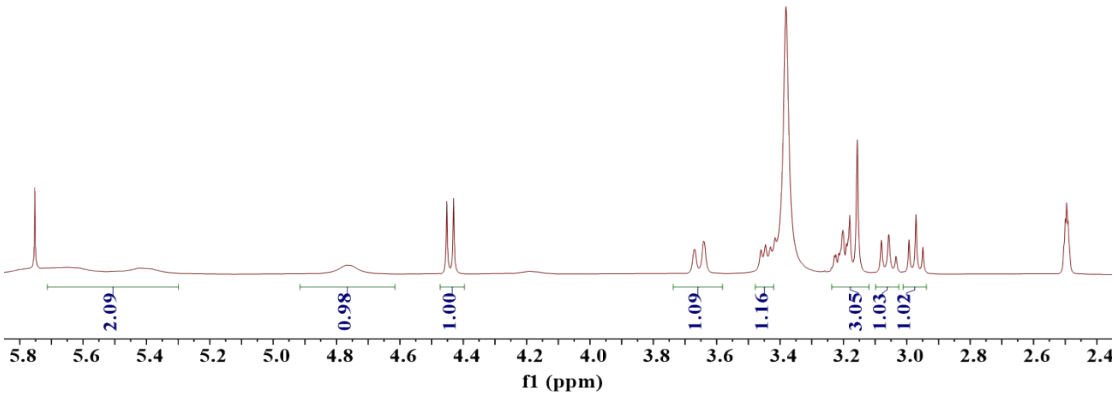

Fig. S4. ^{1}H NMR spectrum of **3** in DMSO-d_6.

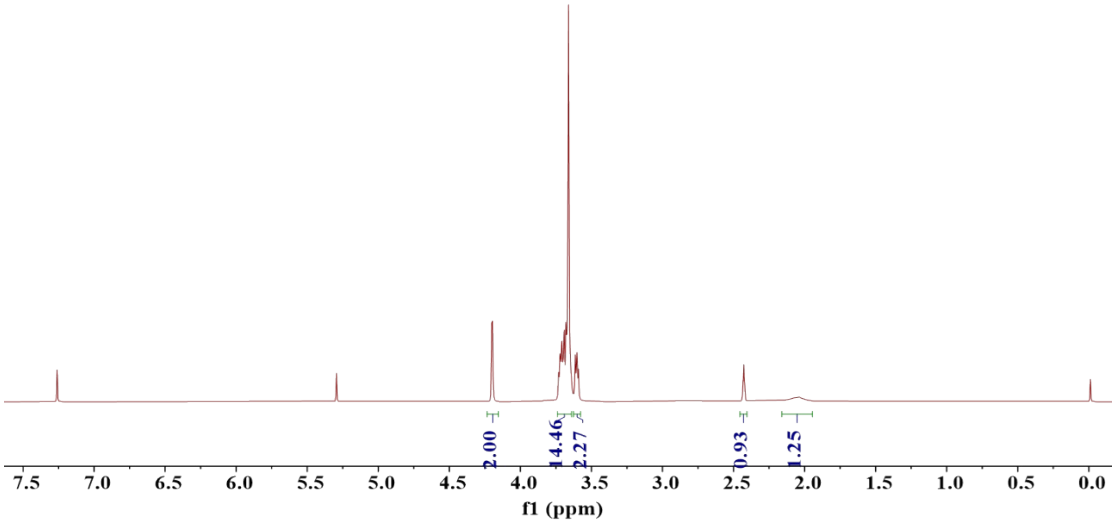

Fig. S5. ^{1}H NMR spectrum of **5** in $CDCl_3$.

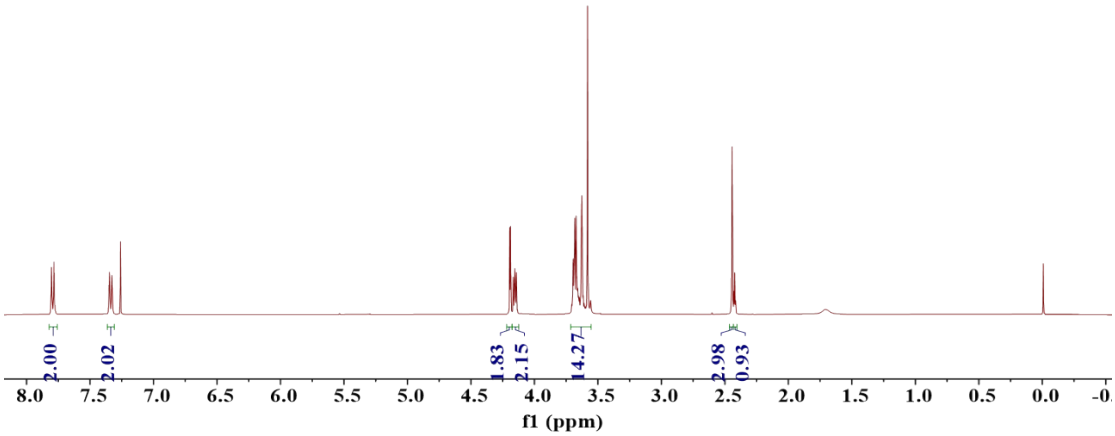

Fig. S6. ^{1}H NMR spectrum of **6** in $CDCl_3$.

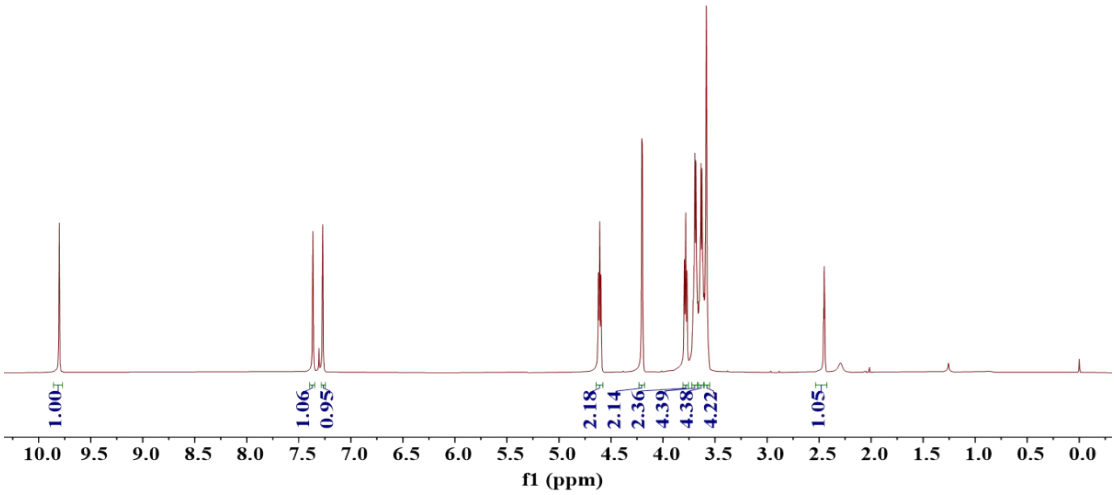

Fig. S7. ^{1}H NMR spectrum of **7** in $CDCl_3$.

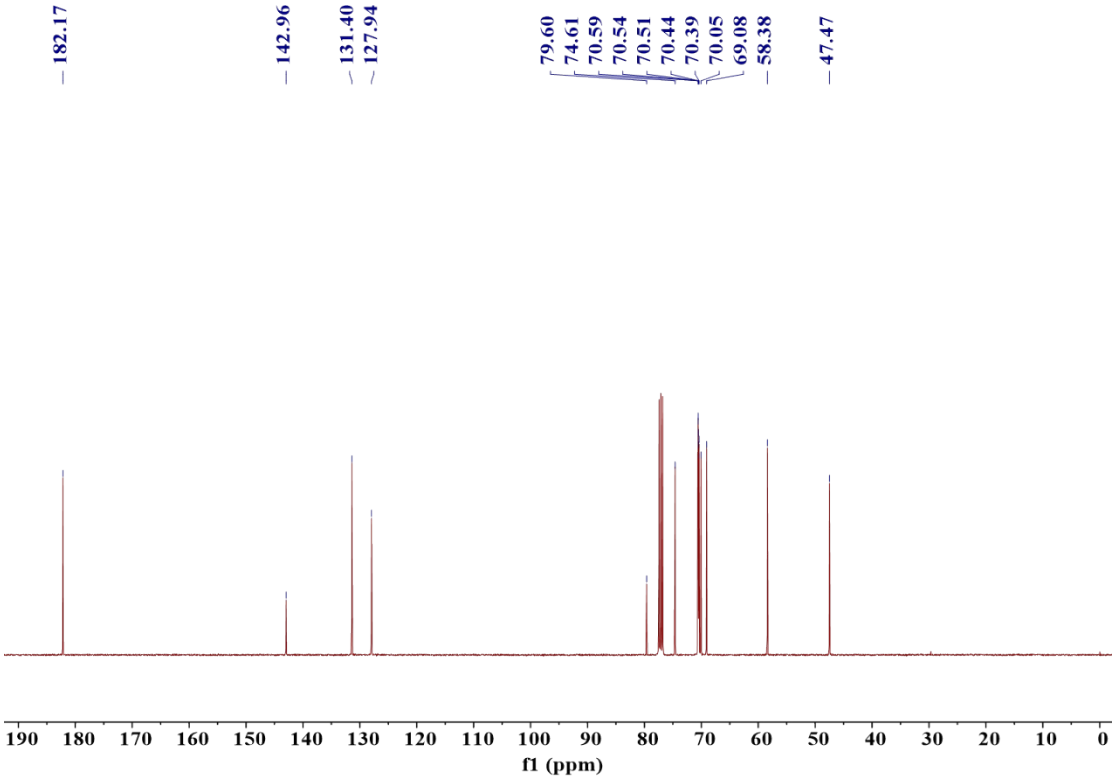

Fig. S8. ^{13}C NMR spectrum of **7** in $CDCl_3$.

Fig. S9. HRMS spectrum of **7**.

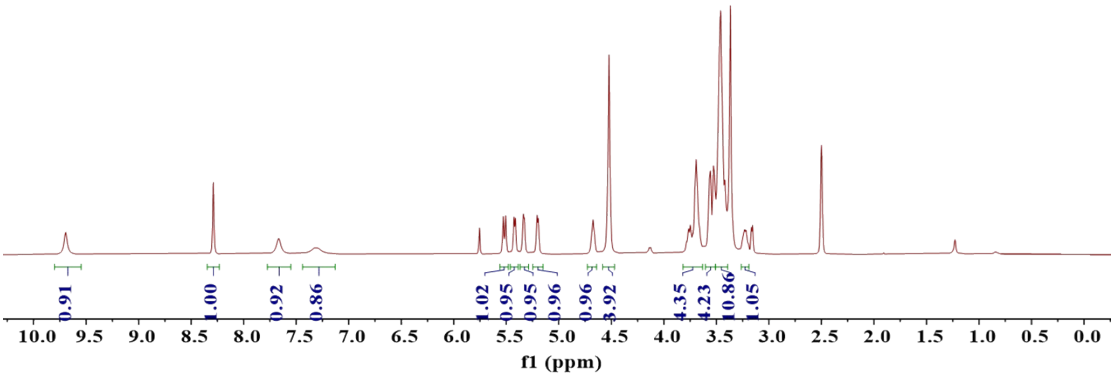

Fig. S10. ^{1}H NMR spectrum of **8** in DMSO-d_6.

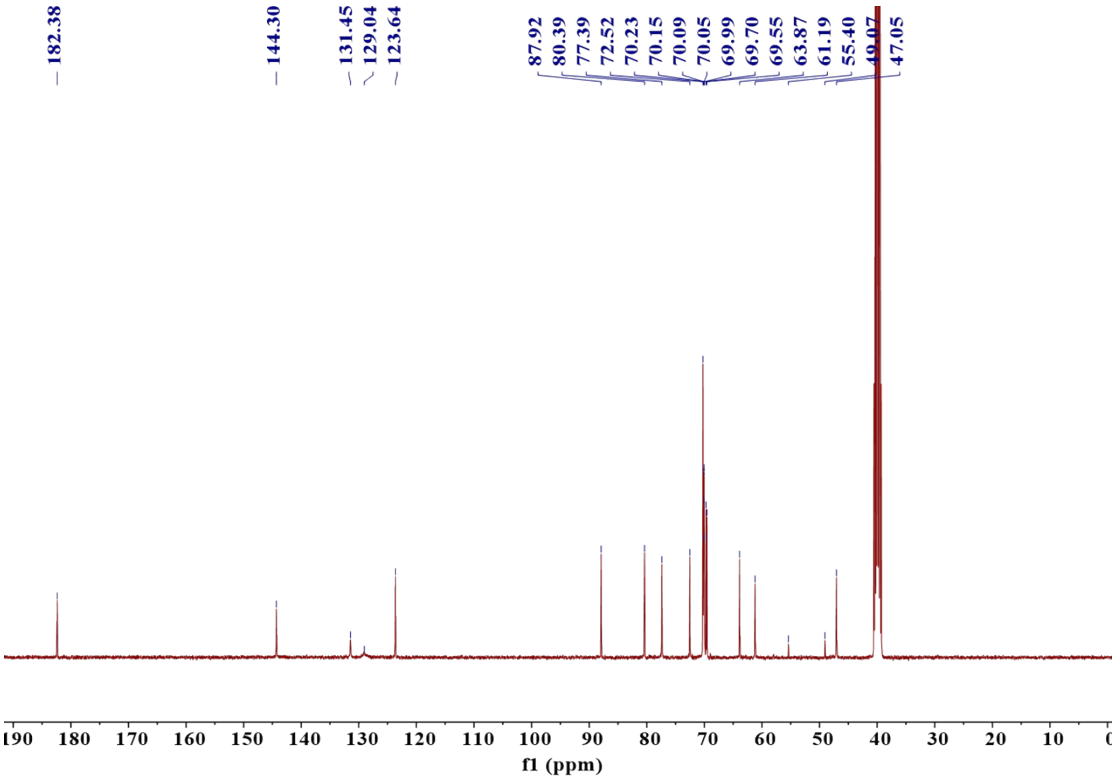

Fig. S11. ^{13}C NMR spectrum of **8** in DMSO-d_6.

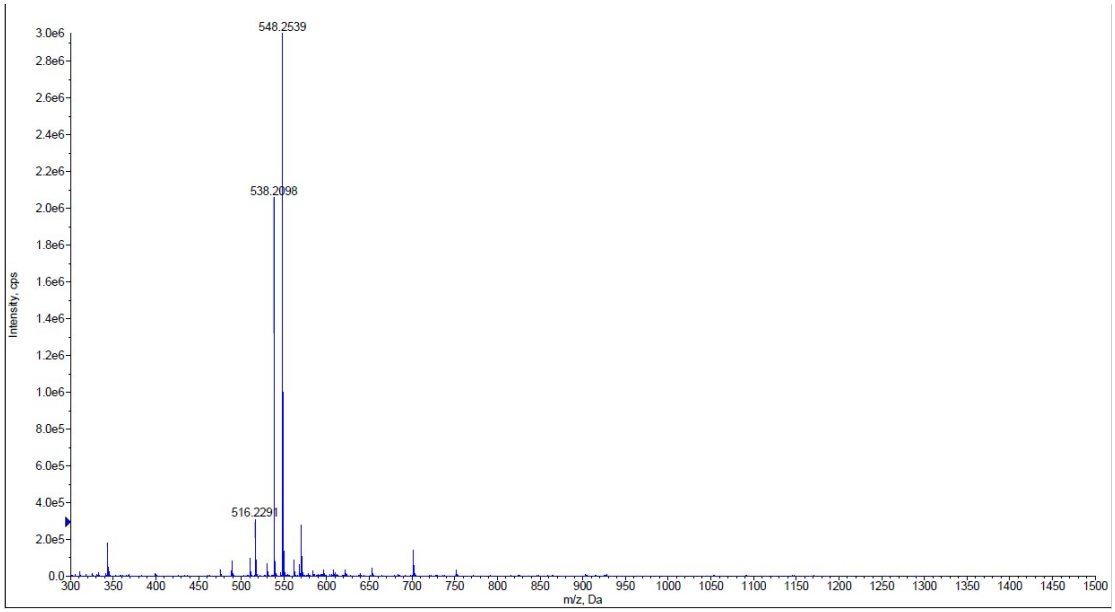

Fig. S12. HRMS spectrum of **8**.

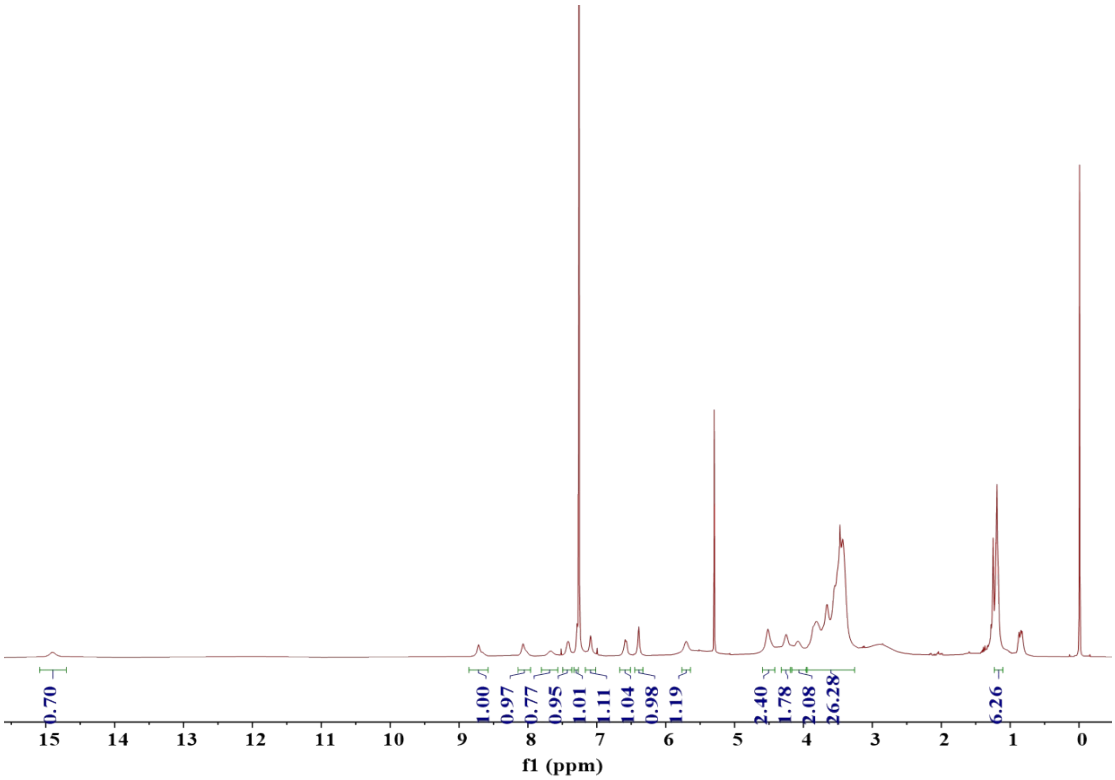

Fig. S13. ^{1}H NMR spectrum of GluC in $CDCl_3$.

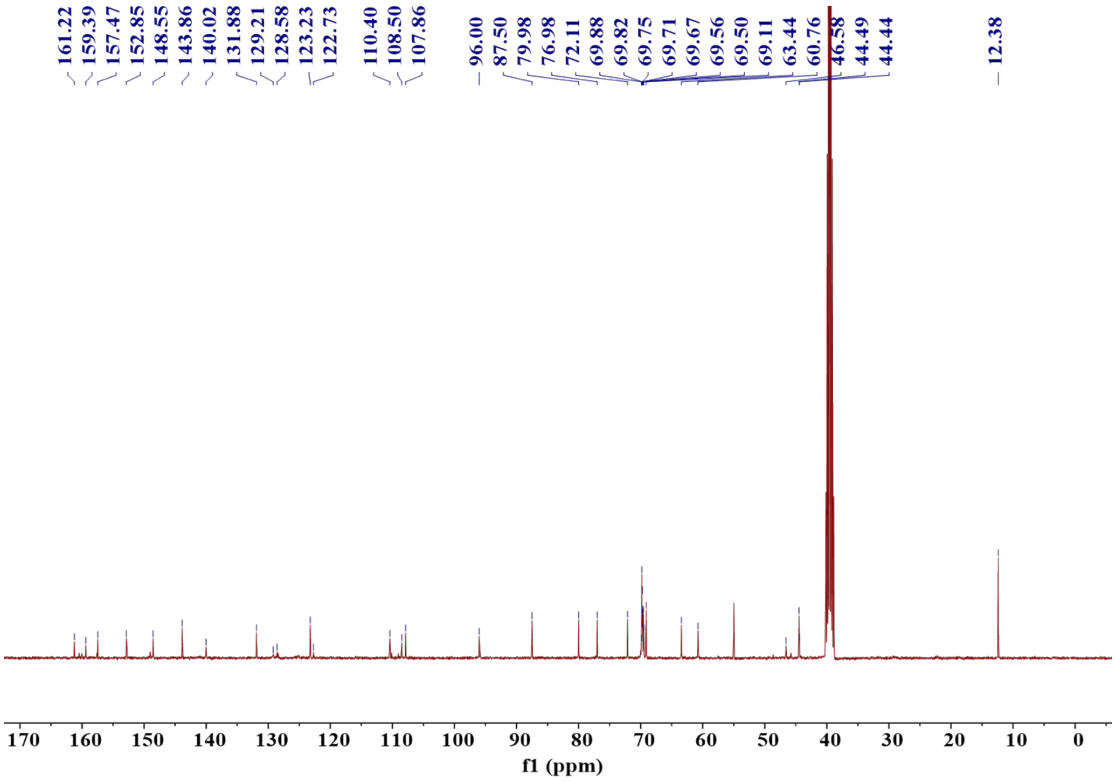

Fig. S14. ^{13}C NMR spectrum of GluC in DMSO-d_6.

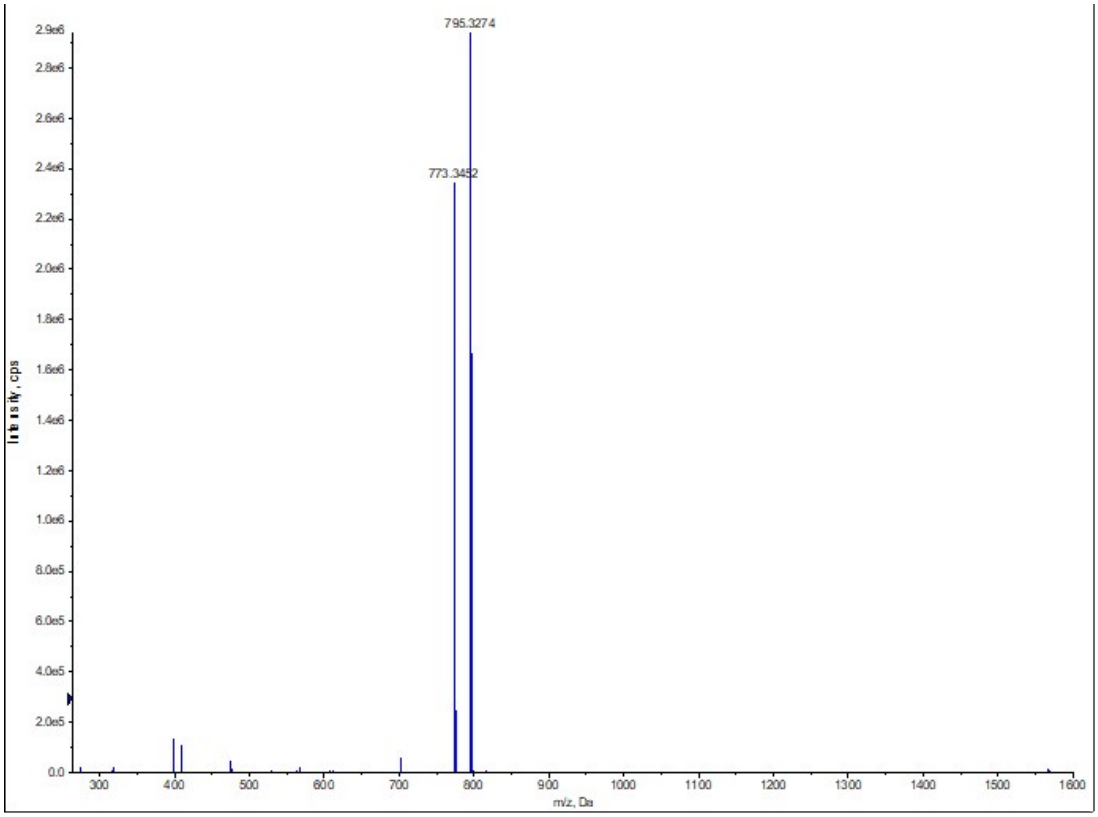

Fig. S15. HRMS spectrum of GluC.

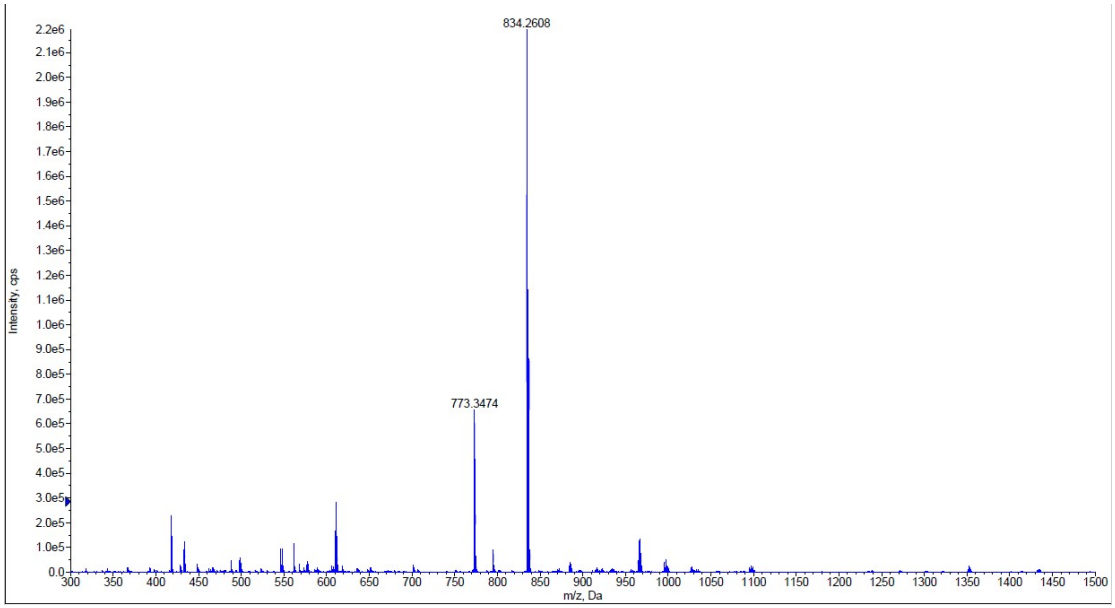

Fig. S16. HRMS spectrum of GluCC.

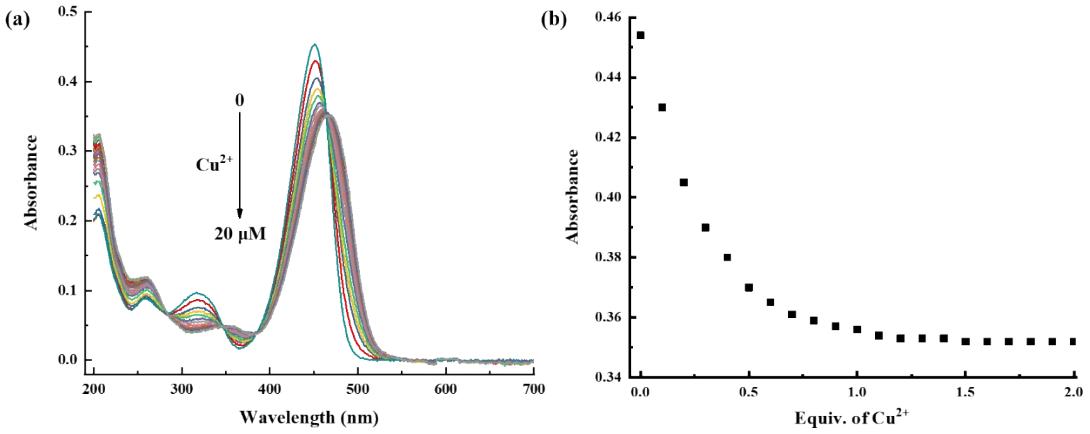

Fig. S17. (a) The UV–vis spectra of GluC (10.0 μM) upon addition of Cu^{2+} (0-2.0 equiv.) in water. (b) Plots of the absorbance of GluC as a function of Cu^{2+} concentration.

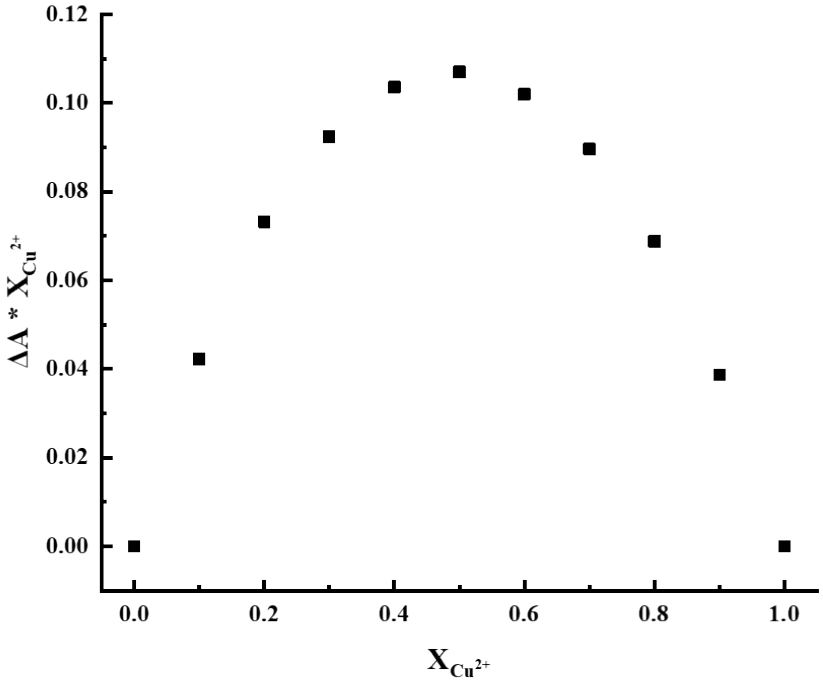

Fig. S18. Job's plot for studying the stoichiometry of GluC and Cu^{2+}.

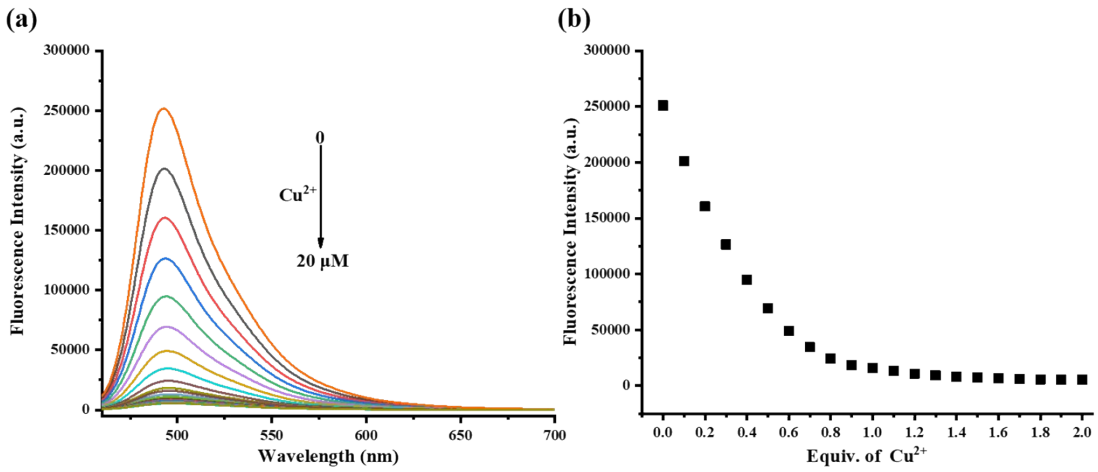

Fig. S19. (a) The fluorescence spectra of GluC (10.0 μM) upon addition of Cu^{2+} (0-2.0 equiv.) in water. (b) Plots of the fluorescence intensity of GluC as a function of Cu^{2+} concentration.

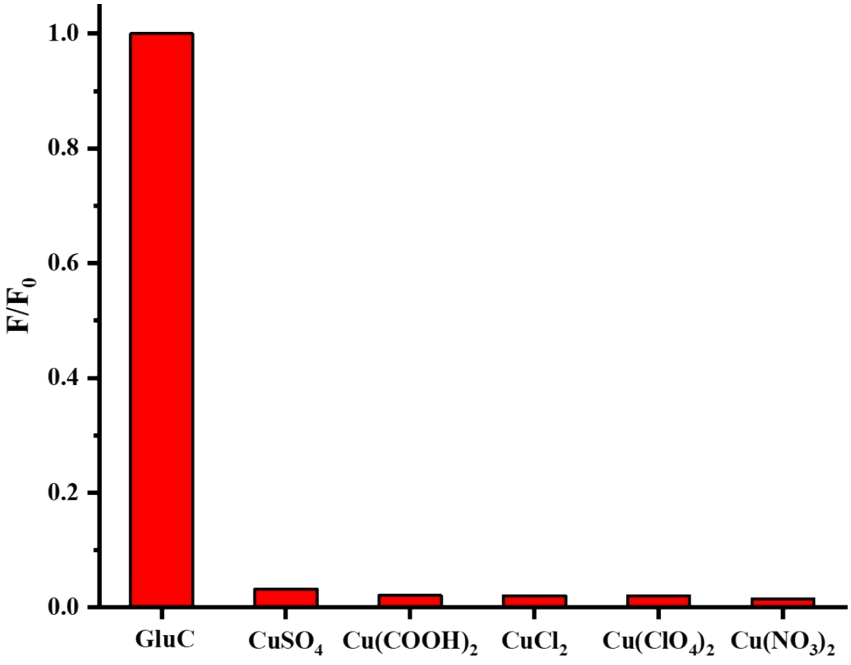

Fig. S20. Fluorescence responses of GluC with $CuSO_4$, $Cu(COOH)_2$, $CuCl_2$, $Cu(ClO_4)_2$ and $Cu(NO_3)_2$ in aqueous solutions.

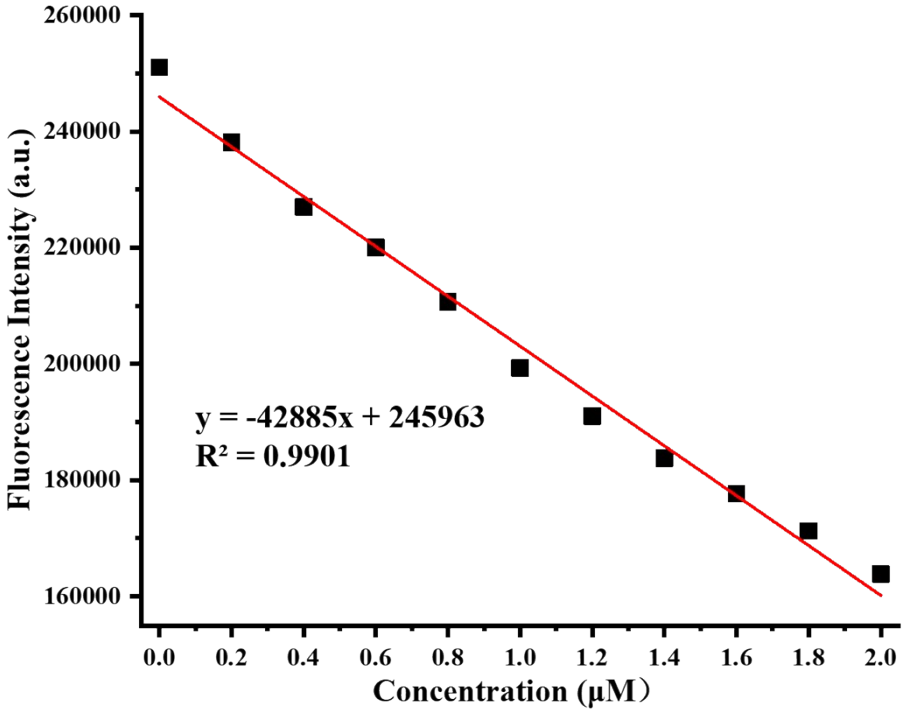

Fig. S21. The linear relationship of the fluorescent intensity (494 nm) of GluC (10.0 μM) relative to the concentration of Cu^{2+} in aqueous solution.

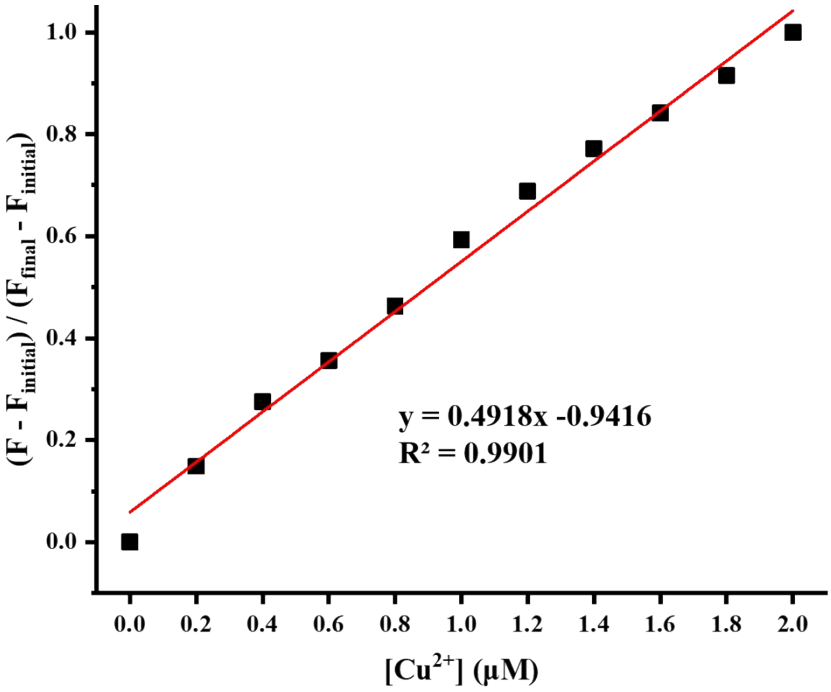

Fig. S22. The linear relationship of the GluC (10.0 μM) fluorescent intensity (at 494 nm) variation relative to the concentration of Cu^{2+} in aqueous solution.

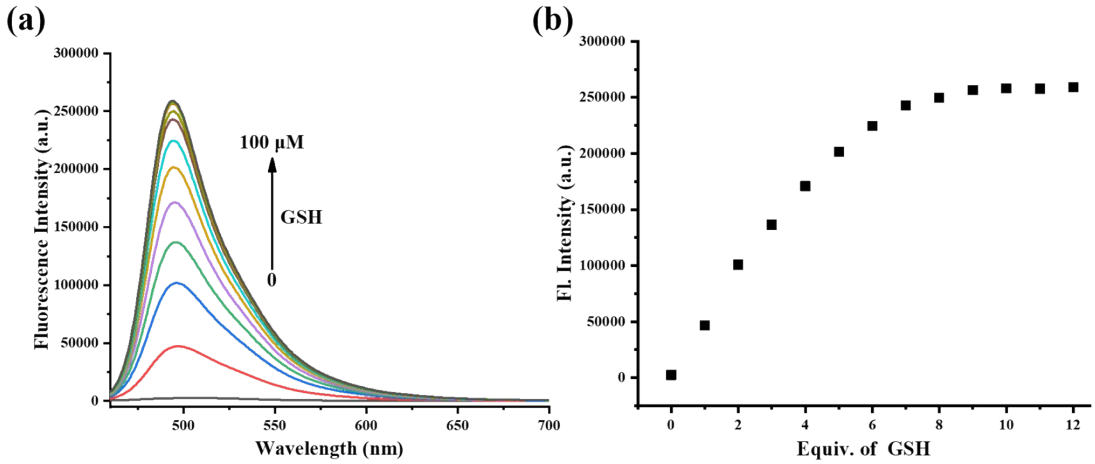

Fig. S23. (a) The fluorescence titration of GluCC (10.0 μM) upon addition of GSH (0-100.0 μM) in aqueous solution; (b) The fluorescence intensity variation of GluCC at 494 nm with increasing equivalent of GSH.

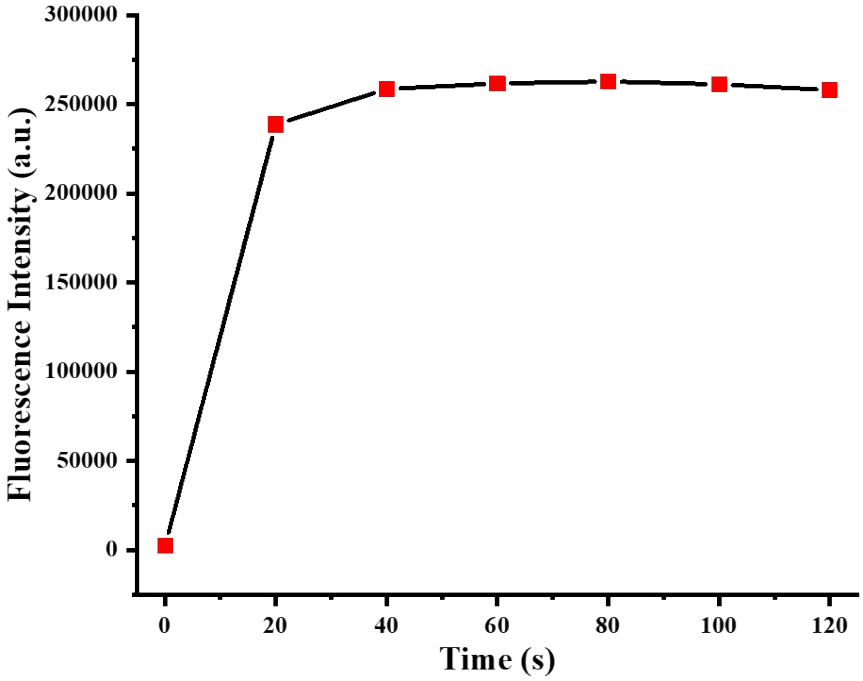

Fig. S24. The time-dependent fluorescence variation process (at 494 nm) of GluCC (10.0 μM) with GSH (100.0 μM) in aqueous solution.

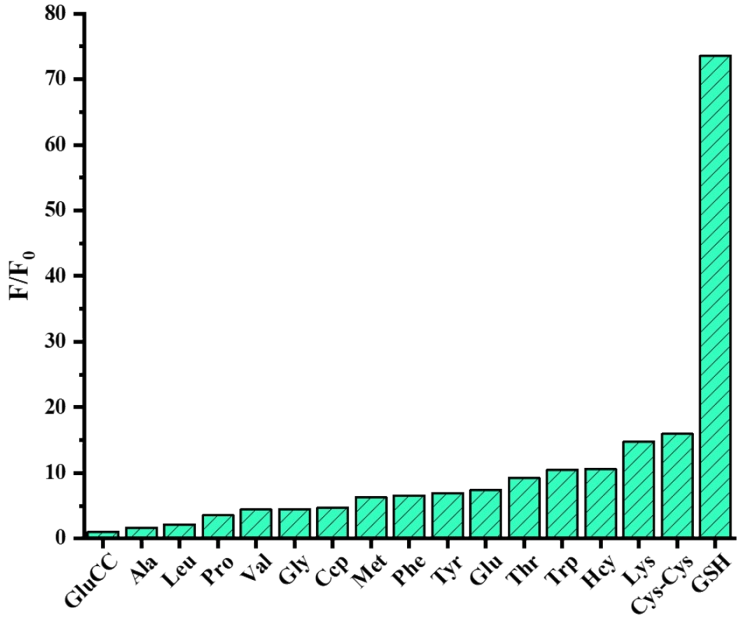

Fig. S25. The fluorescence response of the GluCC (10.0 μM) to different amino acids (100.0 μM).

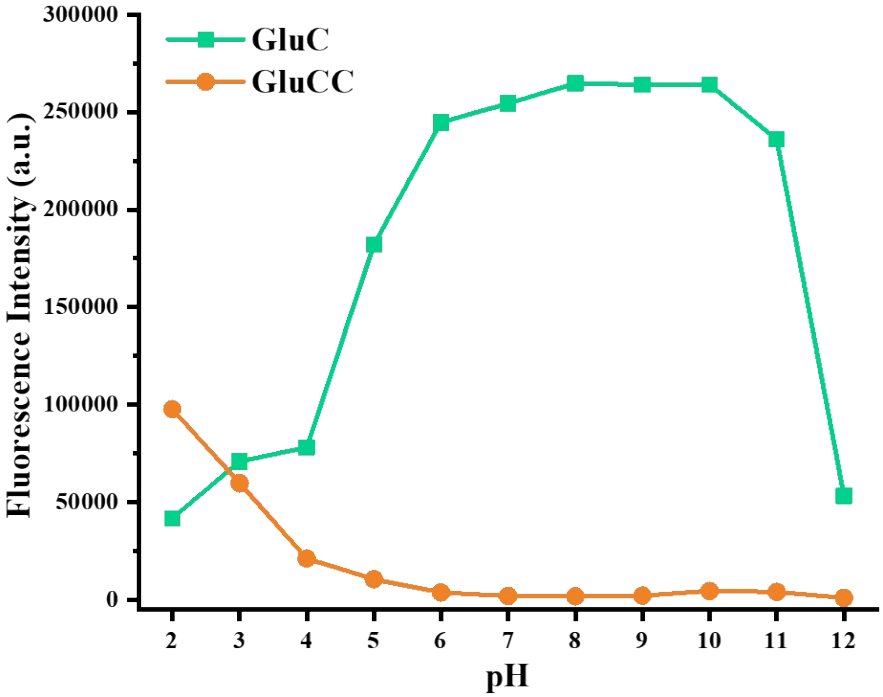

Fig. S26. The pH influence on the fluorescence intensity at 494 nm of GluC (10.0 μM) and GluCC (10.0 μM).

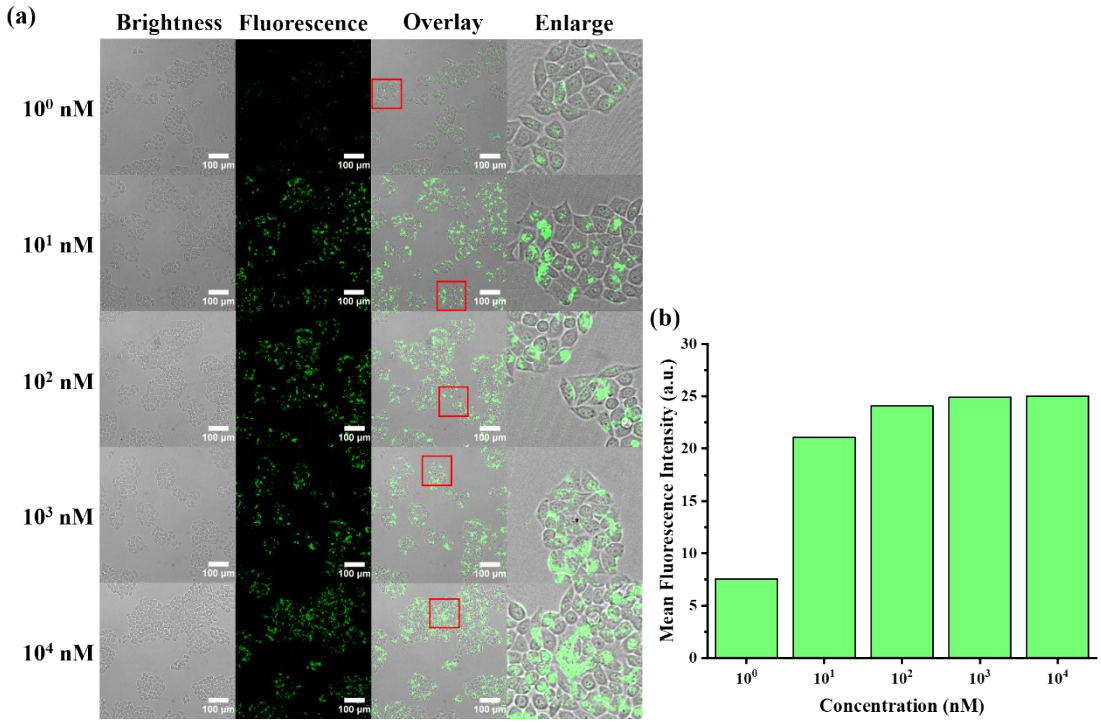

Fig. S27. (a) CLSM images for HepG2 cells incubated with different concentrations of GluCC for 30 min. (b) The mean fluorescence intensity of different concentrations GluCC incubated HepG2 cells.

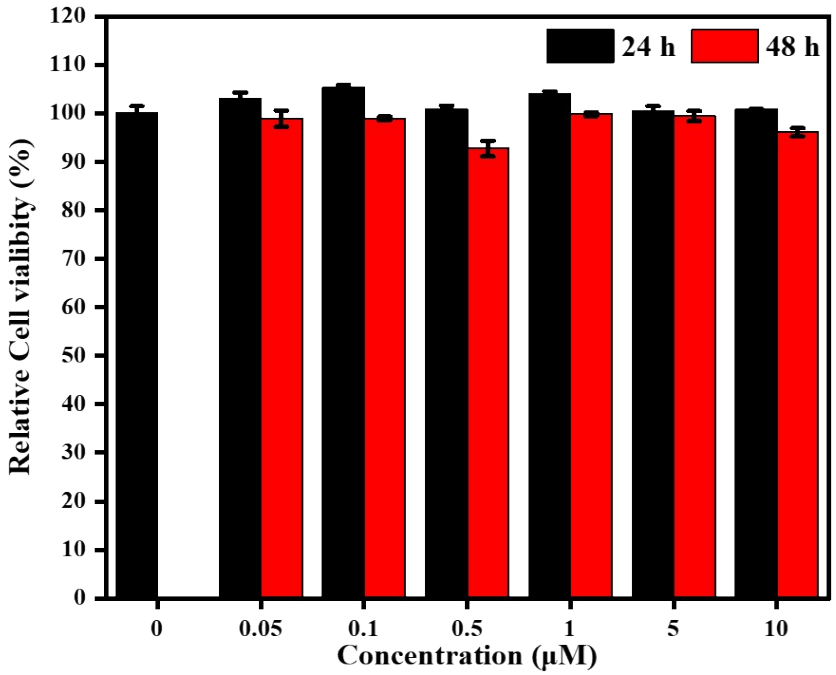

Fig. S28. Relative cell viabilities of HepG2 cells after incubation with different concentrations of GluCC for 24 and 48 h (n = 5).

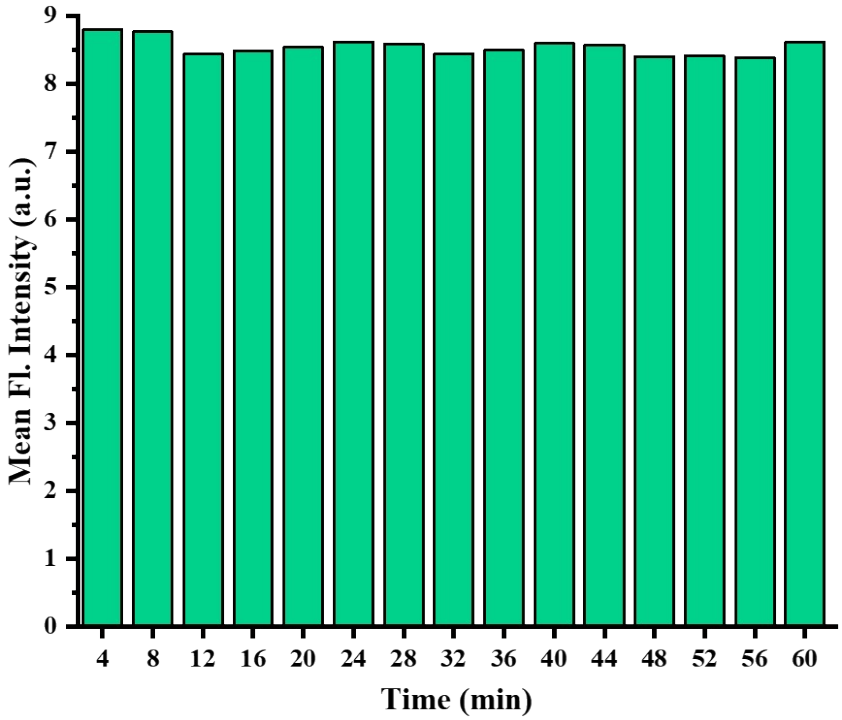

Fig. S29. Mean fluorescence intensity of each image in Fig. 2a.

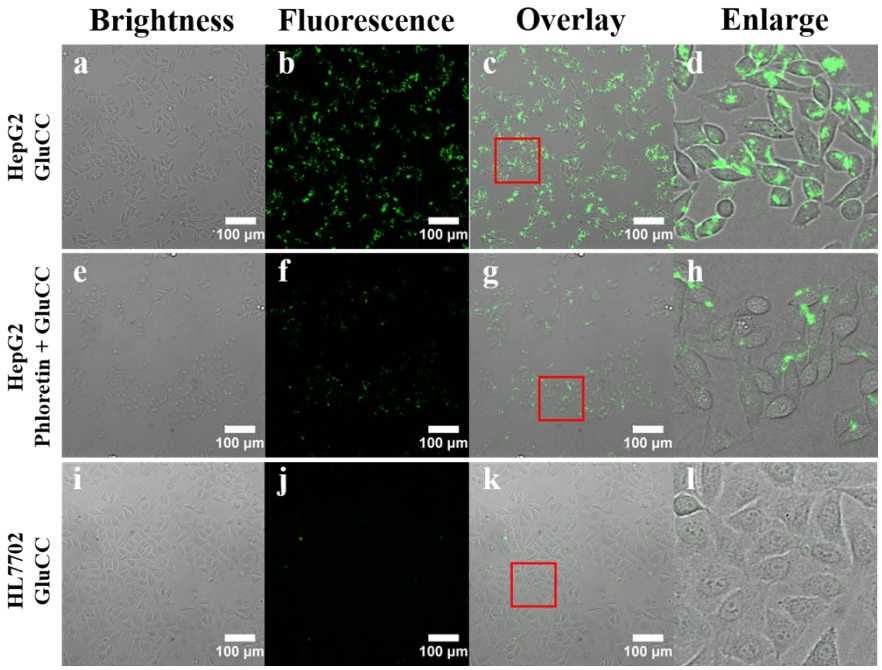

Fig. S30. CLSM images for HepG2 cells incubated with GluCC (10 μM) for 30 min (a-d); HepG2 cells pre-incubated with phloretin (0.2 mM) for 1 h and then cultured with GluCC (10 μM) for 30 min (e-h); HL7702 cells incubated with GluCC (10 μM) for 30 min (i-l).

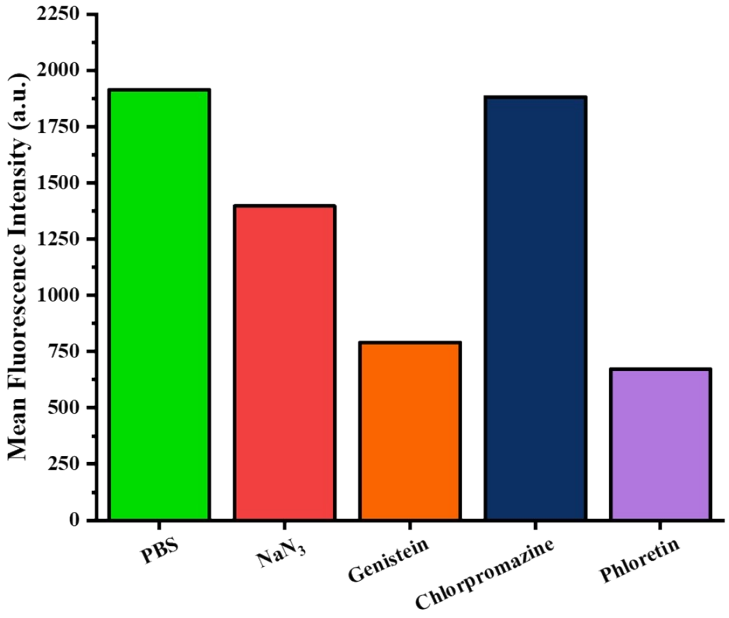

Fig. S31. The mean fluorescence intensity of HepG2 cells incubated with 10 μM GluCC for 30 min in the presence of various endocytosis inhibitors and a GLUTs inhibitor.

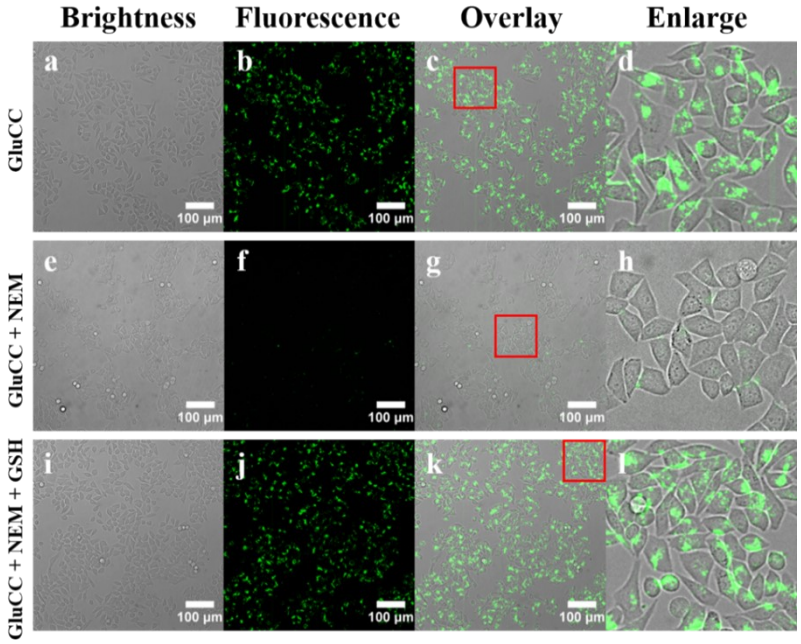

Fig. S32. CLSM images for HepG2 cells incubated with GluCC (10 μM) for 30 min (a-d); HepG2 cells pre-incubated with NEM (1 mM) for 30 min and then treated with GluCC (10 μM) for 30 min (e-h); HepG2 cells pre-incubated with NEM (1 mM) for 30 min and then treated with GSH (2 mM) for 30 min and further incubated with GluCC (10 μM) for 30 min (i-l).

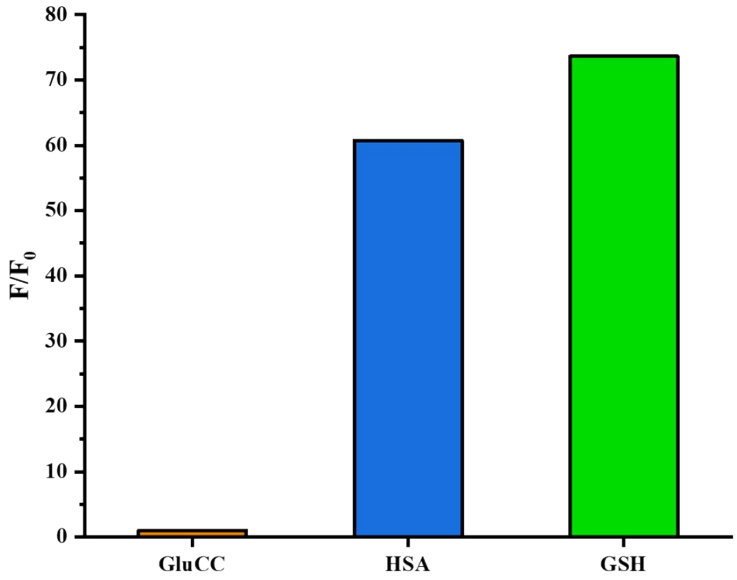

Fig. S33. The fluorescence response of GluCC (10.0 μM) towards HSA (100.0 μM) and GSH (100.0 μM).

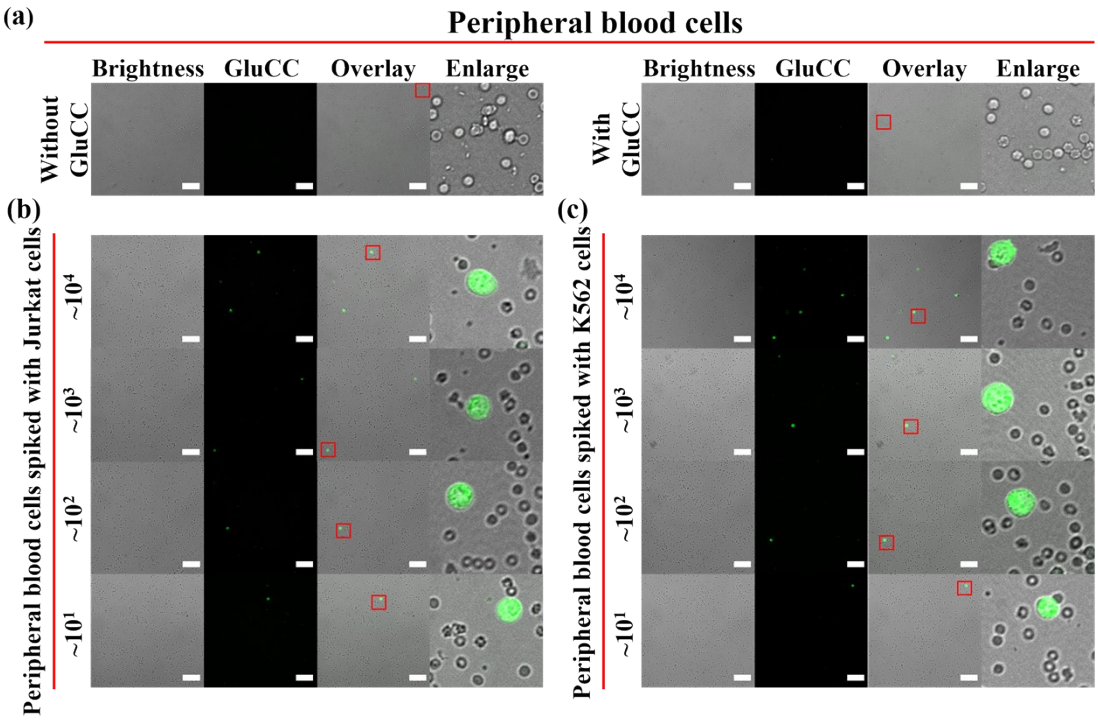

Fig. S34. (a) Peripheral blood cells incubated with or without GluCC (10 μM) for 30 min; different amount of Jurkat cells (b) or K562 cells (c) spiked into peripheral blood then incubated with GluCC (10 μM) for 30 min. The scale bar is 100 μm.

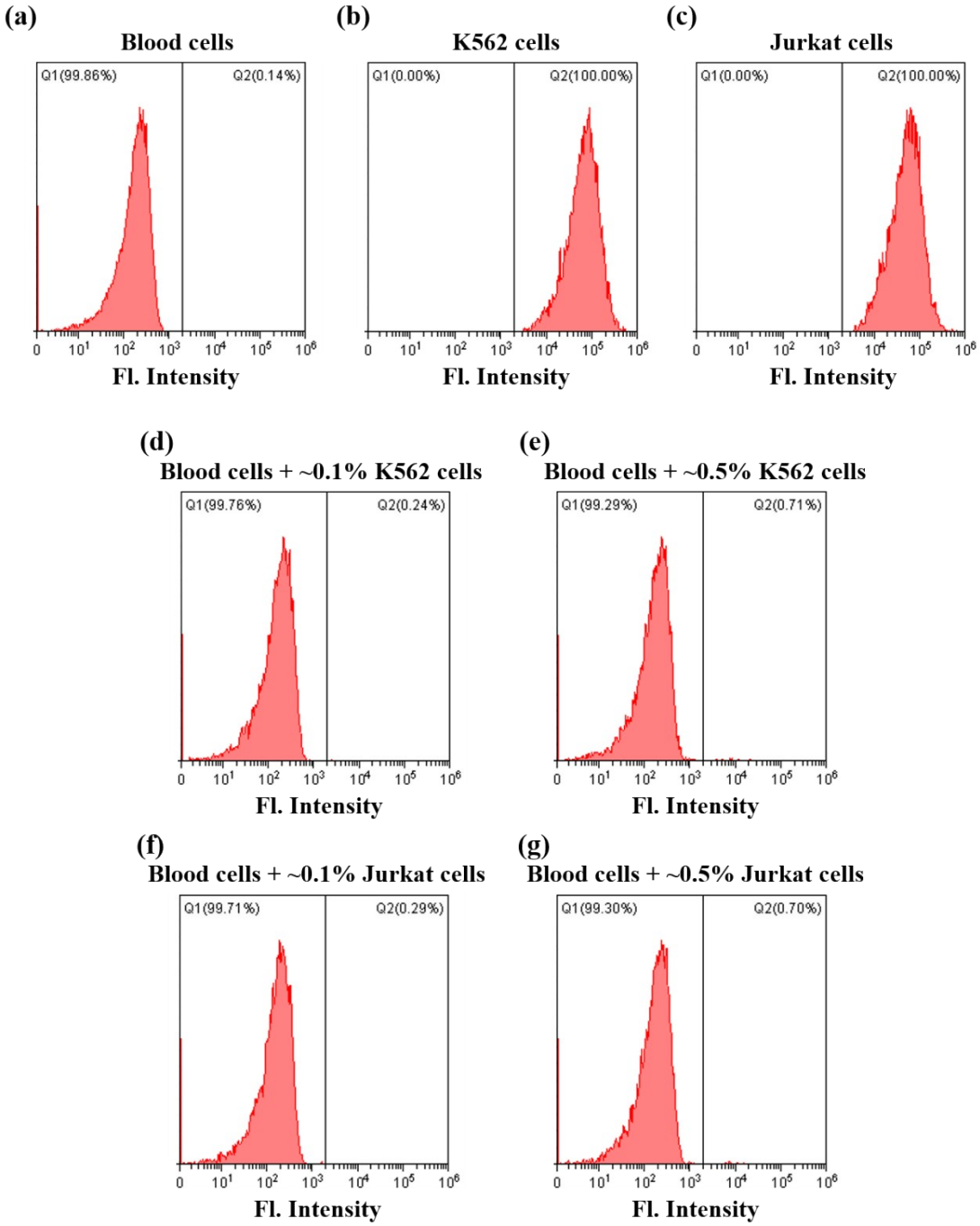

Fig. S35. Flow cytometry analysis of blood cells, K562 cells, Jurkat cells and variable proportions of K562 or Jurkat cells spiked into human peripheral blood (with red blood cells removed) incubated with GluCC (10 μM) for 30 min (with excitation at 405 nm and emission at 450 nm).

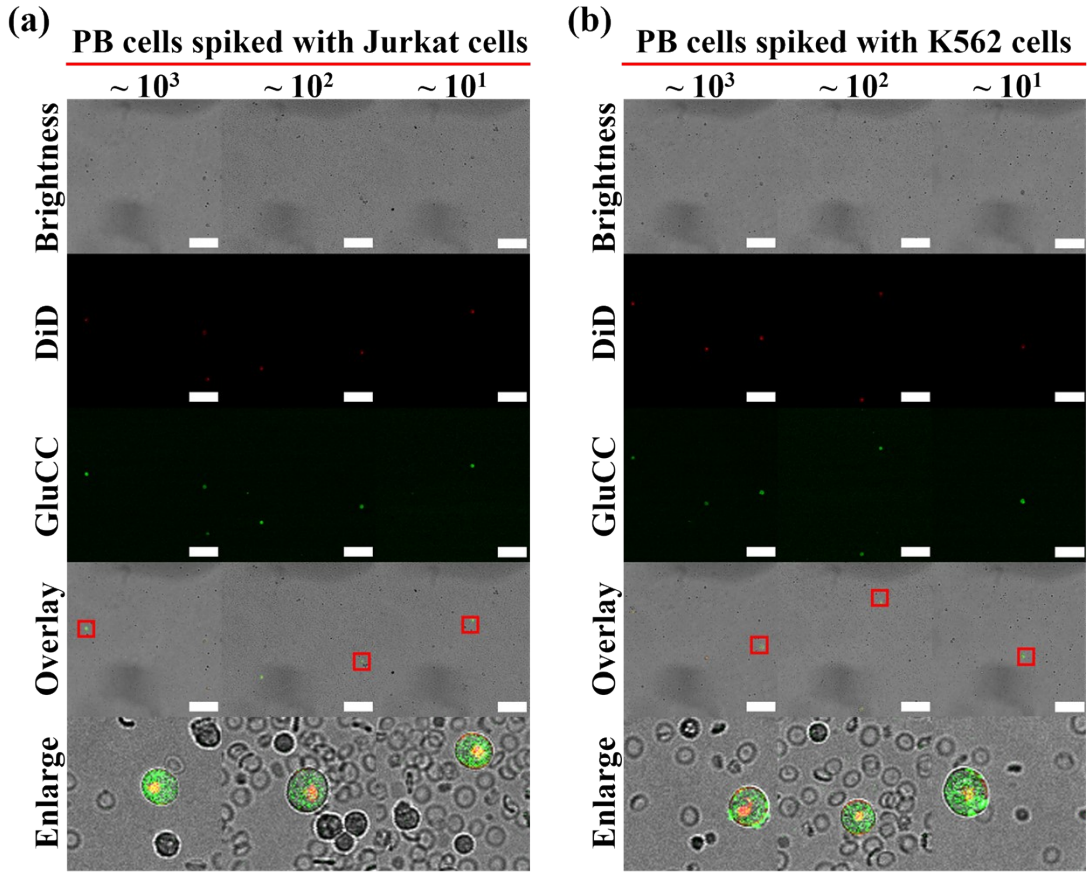

Fig. S36. Different amount of DiD labelled Jurkat cells (a) or K562 cells (b) spiked into human peripheral blood then incubated with GluCC (10 μM) for 30 min. The scale bar is 100 μm.

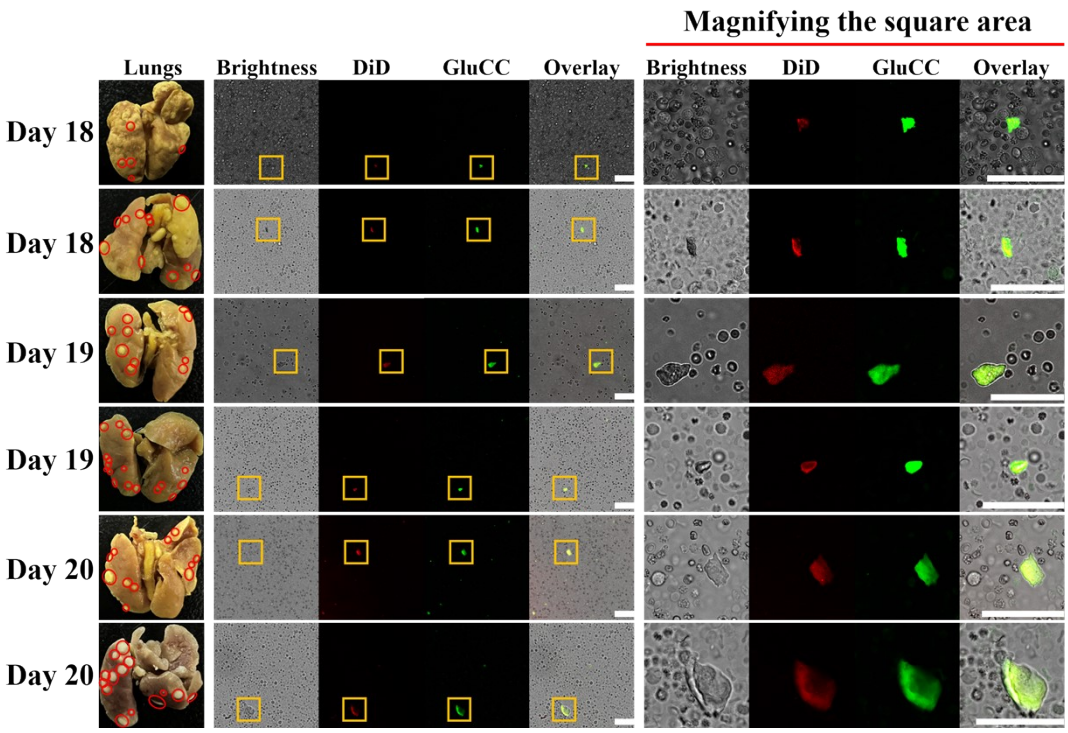

Fig S37. Representative images of lungs collected from lung metastatic mice models on day 18, 19, 20 and CLSM images of lung metastatic mice peripheral blood cells incubated with GluCC (10 μM) for 30 min. The scale bar is 40 μm.

References.

1. G. He, X. Hua, N. Yang, L. Li, J. Xu, L. Yang, Q. Wang and L. Ji, *Bioorg. Chem.*, 2019, **91**, 103176.
2. M. Pintal, F. Charbonniere-Dumarcay, A. Marsura and S. Porwanski, *Carbohydr. Res.*, 2015, **414**, 51-59.
3. S. Zhu, J. Zhang, G. Vegesna, F. T. Luo, S. A. Green and H. Liu, *Org. Lett.*, 2011, **13**, 438-441.
4. D. E. Kang, C. S. Lim, J. Y. Kim, E. S. Kim, H. J. Chun and B. R. Cho, *Anal. Chem.*, 2014, **86**, 5353-5359.
5. K. Jiang, S. Sun, L. Zhang, Y. Lu, A. Wu, C. Cai and H. Lin, *Angew Chem Int Ed Engl*, 2015, **54**, 5360-5363.
6. L. Wang, Y. Yu, D. Wei, L. Zhang, X. Zhang, G. Zhang, D. Ding, H. Xiao and D. Zhang, *Adv. Mater.*, 2021, **33**, e2100599; L. Zhang, S.-S. Wan, C.-X. Li, L. Xu, H. Cheng and X.-Z. Zhang, *Nano Lett.*, 2018, **18**, 7609-7618.
7. K. Luo, Y. Gao, S. Yin, Y. Yao, H. Yu, G. Wang and J. Li, *Acta Biomater.*, 2021, **134**, 649-663; J. Shi, Y. Ren, J. Ma, X. Luo, J. Li, Y. Wu, H. Gu, C. Fu, Z. Cao and J. Zhang, *J Nanobiotechnology*, 2021, **19**, 188; L. Luo, F. Xu, H. Peng, Y. Luo, X. Tian, G. Battaglia, H. Zhang, Q. Gong, Z. Gu and K. Luo, *J. Control. Release*, 2020, **318**, 124-135.
8. D. A. Sipkins, X. Wei, J. W. Wu, J. M. Runnels, D. Cote, T. K. Means, A. D. Luster, D. T. Scadden and C. P. Lin, *Nature*, 2005, **435**, 969-973; J. Fujisaki, J. Wu, A. L. Carlson, L.

Silberstein, P. Putheti, R. Larocca, W. Gao, T. I. Saito, C. Lo Celso, H. Tsuyuzaki, T. Sato, D. Cote, M. Sykes, T. B. Strom, D. T. Scadden and C. P. Lin, *Nature*, 2011, **474**, 216-219.